

Ab initio theory of spin-dependent conductivity tensor and spin Hall effect in random alloys

I. Turek*

Institute of Physics of Materials, Academy of Sciences of the Czech Republic, Žižkova 22, CZ-616 62 Brno, Czech Republic

J. Kudrnovský† and V. Drchal‡

Institute of Physics, Academy of Sciences of the Czech Republic,

Na Slovance 2, CZ-182 21 Praha 8, Czech Republic

(Dated: December 15, 2024)

We present an extension of the relativistic electron transport theory for the standard (charge) conductivity tensor of random alloys within the tight-binding linear muffin-tin orbital method to the so-called spin-dependent conductivity tensor, which describes the Kubo linear response of spin currents to external electric fields. The approach is based on effective charge- and spin-current operators, that correspond to intersite electron transport and that are nonrandom, which simplifies the configuration averaging by means of the coherent potential approximation. Special attention is paid to the Fermi sea term of the spin-dependent conductivity tensor, which contains a nonzero incoherent part, in contrast to the standard conductivity tensor. The developed formalism is applied to the spin Hall effect in binary random nonmagnetic alloys, both on a model level and for Pt-based alloys with an fcc structure. We show that the spin Hall conductivity consists of three contributions (one intrinsic and two extrinsic) which exhibit different concentration dependences in the dilute limit of an alloy. Results for selected Pt alloys (Pt-Re, Pt-Ta) lead to the spin Hall angles around 0.2; these sizeable values are obtained for compositions that belong to thermodynamically equilibrium phases. These alloys can thus be considered as an alternative to other systems for efficient charge to spin conversion, which are often metastable crystalline or amorphous alloys.

I. INTRODUCTION

Efficient generation and reliable detection of spin currents in magnetoelectronic devices belong to the central topics of the whole area of spintronics^{1,2}. In systems without local magnetic moments and in absence of external magnetic fields, the most important phenomenon in this context is undoubtedly the spin Hall effect (SHE)³. This transport phenomenon was predicted as a consequence of spin-orbit interaction⁴; subsequent systematic theoretical and experimental investigation resulted in detailed understanding of its basic aspects.

In pure metals and ordered crystals, the SHE arises solely due to the band structure of the system, i.e., due to the dependence of energy eigenvalues and eigenvectors on the reciprocal-space vector \mathbf{k} , without the need of any explicit mechanism of electron scattering. The central quantity, namely, the intrinsic spin Hall conductivity (SHC), can be expressed in terms of the Berry curvature of the occupied electron states^{5,6}. In diluted metallic alloys, the impurity scattering leads to an extrinsic contribution to the SHC, that can be treated on different levels of sophistication of electron transport theory. The extrinsic SHC is due to a skew-scattering mechanism; its evaluation within the linearized Boltzmann equation rests on the scattering-in terms⁷ while the Kubo linear response theory with the coherent potential approximation (CPA) requires inclusion of the so-called vertex corrections⁸.

The intrinsic and extrinsic contributions to the SHC have its counterparts in a description of the anomalous Hall effect in ferromagnetic systems^{9,10}, so that similar concepts appear in studies of both transverse transport phenomena. In the SHE, the relative magnitude of the SHC is expressed by the so-called spin Hall angle (SHA), defined as a ratio of the SHC to the standard (charge) longitudinal conductivity. The SHA represents a dimensionless measure of efficiency of the charge to spin conversion. For this reason, both experimental and theoretical effort has recently been devoted to find systems with large SHA, see, e.g., Refs. 11 and 12 and references therein. Besides the usual bulk metals and diluted and concentrated alloys containing heavy elements, especially large SHA values can be induced by interface effects where the nonmagnetic system is placed in a contact with a ferromagnet¹³. Further manifestation of spin-orbit effects in nonmagnetic solids is a possible spin polarization of longitudinal currents due to a special point group symmetry of the crystal structure¹⁴.

Spin currents in systems with spontaneous magnetic moments represent another wide area of the present intense research. This field includes spin-transfer torques in layered systems¹⁵, spin polarization of longitudinal¹⁶ and transversal¹⁰ conductivities in bulk ferromagnetic alloys, as well as the SHE in collinear⁶ and noncollinear¹⁷ antiferromagnets. The latter systems have attracted special interest since their noncollinear spin structures can induce a sizeable SHE even without spin-orbit interaction¹⁸.

Reliable quantum-mechanical description of phenomena related to the spin currents faces a basic problem due to the fact that the electron spin in systems with spin-orbit interaction is not a conserving quantity. This hinders an

exact definition of the spin-current operator; fundamental approaches to this problem^{19,20} lead to expressions that cannot be employed directly in current *ab initio* techniques of electron theory of solids. In this situation, existing practical solutions thus express the spin-current operator typically as a symmetrized product of the spin operator and the operator of charge current^{5,13,16}. It should be noted that the latter approaches are suitable even for studies of disordered systems, in which the necessary configuration averaging is performed either by a real-space supercell technique¹³ or by using the CPA^{8,16}.

The main aim of this work is a formulation of an alternative first-principles approach to the spin currents in random alloys which employs the idea of an intersite electron transport²¹. In this scheme, the intraatomic electron motion is systematically neglected which leads to effective operators of charge current that are spin-independent and nonrandom (independent of a particular random configuration of the alloy). The corresponding effective spin-current operators are nonrandom as well, which allows us to define easily the spin-dependent conductivity tensor and to perform its configuration averaging within the single-site CPA^{22,23} in analogy with the technique developed recently for the standard (charge) conductivity tensor in relativistic theory^{24,25}.

The paper is organized as follows. The theoretical formalism is presented in Section II, including the definition of the spin-dependent conductivity tensor (Section II A), the CPA-averaging of its Fermi sea term (Section II B), a summary of the formal properties of the derived theory (Section II C), and details of numerical implementation (Section II D). Technical theoretical details are presented in Appendix A. The obtained results and their discussion, focused on the SHE in nonmagnetic random alloys, are collected in Section III. First, a simple tight-binding model of a random binary alloy is analysed in the dilute limit in Section III A. Second, transport properties of selected Pt-based disordered fcc alloys (Pt-Au, Pt-Re, Pt-Ta) are addressed in Section III B. Conclusions of the work are summarized in Section IV.

II. METHOD

A. Spin-dependent conductivity tensor from the Bastin formula

The starting point of our formalism is the Kubo linear response theory²⁶ and the formula of Bastin et al.²⁷ for the full charge conductivity tensor $\sigma_{\mu\nu}$ adapted in the relativistic tight-binding linear muffin-tin orbital (TB-LMTO) method²⁵

$$\sigma_{\mu\nu} = -2\sigma_0 \int dE f(E) \text{Tr} \langle v_\mu g'_+(E) v_\nu [g_+(E) - g_-(E)] \\ - v_\mu [g_+(E) - g_-(E)] v_\nu g'_-(E) \rangle. \quad (1)$$

In this relation, the quantity $\sigma_0 = e^2 \hbar / (4\pi\Omega)$, where Ω is the volume of a big finite crystal with periodic boundary conditions, E is a real energy variable, $f(E)$ denotes the Fermi-Dirac function, $g_\pm(E) = g(E \pm i0)$ denote side limits of the auxiliary Green's function $g(z)$ defined for complex energies z , the prime at $g_\pm(E)$ denotes energy derivative, the quantities v_μ ($\mu = x, y, z$) are the effective velocity (current) operators, and the brackets $\langle \dots \rangle$ refer to the configuration averaging for random alloys. The auxiliary Green's function is given as $g(z) = [P(z) - S]^{-1}$, where $P(z)$ represents a site-diagonal matrix of the potential functions and S denotes the structure constant matrix.

The expression (1) reflects the intersite electron transport which takes place inside the interstitial region among the individual Wigner-Seitz cells (replaced by space-filling spheres in the atomic-sphere approximation). The operators v_μ and $g_\pm(E)$ are represented by matrices in the composed index $\mathbf{R}L$, where \mathbf{R} labels the lattice sites and L denotes the orbital index $L = (\ell m s)$ containing the orbital (ℓ), magnetic (m), and spin (s) quantum numbers ($s = \uparrow, \downarrow$). The trace (Tr) in Eq. (1) refers to all $\mathbf{R}L$ -orbitals of the system. Note that the orbital index L corresponds to a nonrelativistic theory despite the fully relativistic solutions (including possible spin polarization) of the single-site problem are used inside the Wigner-Seitz cells (atomic spheres); this fact is due to the nonrelativistic form of the LMTO-orbitals in the interstitial region (which reduce to spherical waves in a constant potential with zero kinetic energy^{28,29}). The effective current operators v_μ are spin-independent and nonrandom which follows from their definition^{21,25} and from properties of the structure constant matrix S .

The nonrelativistic character of the intersite electron transport and the above properties of the effective current operators v_μ allow one to introduce naturally the effective spin-current operators as $\sigma^\lambda v_\mu$, where the quantities σ^λ ($\lambda = x, y, z$) equal the Pauli spin matrices extended trivially to matrices in the composed $\mathbf{R}L$ -index, $(\sigma^\lambda)_{\mathbf{R}'\mathbf{R}}^{L'L} = \delta_{\mathbf{R}'\mathbf{R}} \delta_{\ell'\ell} \delta_{m'm} \sigma_{s's}^\lambda$ where $L' = (\ell' m' s')$. This definition represents an analogy of spin-current operators employed in other studies^{5,13,16}. The spin-dependent conductivity tensor $\sigma_{\mu\nu}^\lambda$ corresponding to the original charge conductivity tensor (1) is then defined by

$$\sigma_{\mu\nu}^\lambda = -2\sigma_0 \int dE f(E) \text{Tr} \langle (\sigma^\lambda v_\mu) g'_+(E) v_\nu [g_+(E) - g_-(E)] \\ - v_\mu [g_+(E) - g_-(E)] v_\nu g'_-(E) \rangle$$

$$- (\sigma^\lambda v_\mu) [g_+(E) - g_-(E)] v_\nu g'_-(E) \rangle, \quad (2)$$

which describes the linear response of the spin current $\sigma^\lambda v_\mu$ to a spin-independent electrical field in direction of ν axis. Alternatively, one can consider the response coefficient

$$\begin{aligned} \tilde{\sigma}_{\mu\nu} = -2\sigma_0 \int dE f(E) \text{Tr} & \langle \tilde{v}_\mu g'_+(E) v_\nu [g_+(E) - g_-(E)] \\ & - \tilde{v}_\mu [g_+(E) - g_-(E)] v_\nu g'_-(E) \rangle, \end{aligned} \quad (3)$$

where $\tilde{v}_\mu = (\mathbf{n} \cdot \boldsymbol{\sigma}) v_\mu$ denotes the spin-polarized effective velocity (current) with the spin-polarization axis along a global nonrandom unit vector \mathbf{n} . Note that the spin-polarized velocities \tilde{v}_μ are nonrandom operators, which simplifies the configuration averaging in Eq. (3).

In full analogy to $\sigma_{\mu\nu}$, the spin-dependent conductivity tensor $\tilde{\sigma}_{\mu\nu}$ can be decomposed into a Fermi surface term and a Fermi sea term as^{25,30}

$$\tilde{\sigma}_{\mu\nu} = \tilde{\sigma}_{\mu\nu}^{(1)} + \tilde{\sigma}_{\mu\nu}^{(2)}. \quad (4)$$

For systems at zero temperature, the Fermi surface term $\tilde{\sigma}_{\mu\nu}^{(1)}$ can be written as

$$\begin{aligned} \tilde{\sigma}_{\mu\nu}^{(1)} = \sigma_0 \text{Tr} & \langle \tilde{v}_\mu [g_+(E_F) - g_-(E_F)] v_\nu g_-(E_F) \\ & - \tilde{v}_\mu g_+(E_F) v_\nu [g_+(E_F) - g_-(E_F)] \rangle, \end{aligned} \quad (5)$$

where E_F denotes the Fermi energy. The Fermi sea term $\tilde{\sigma}_{\mu\nu}^{(2)}$ can be reformulated as a complex contour integral

$$\tilde{\sigma}_{\mu\nu}^{(2)} = \sigma_0 \int_C dz \text{Tr} \langle \tilde{v}_\mu g'(z) v_\nu g(z) - \tilde{v}_\mu g(z) v_\nu g'(z) \rangle, \quad (6)$$

where the integration path C starts and ends at E_F , it is oriented counterclockwise and it encompasses the whole occupied part of the alloy valence spectrum.

The configuration average in the CPA of the Fermi surface term yields its coherent part (coh) and the incoherent part (vertex corrections – VC), $\tilde{\sigma}_{\mu\nu}^{(1)} = \tilde{\sigma}_{\mu\nu,coh}^{(1)} + \tilde{\sigma}_{\mu\nu,VC}^{(1)}$, where

$$\begin{aligned} \tilde{\sigma}_{\mu\nu,coh}^{(1)} = \sigma_0 \text{Tr} & \{ \tilde{v}_\mu [\bar{g}_+(E_F) - \bar{g}_-(E_F)] v_\nu \bar{g}_-(E_F) \\ & - \tilde{v}_\mu \bar{g}_+(E_F) v_\nu [\bar{g}_+(E_F) - \bar{g}_-(E_F)] \}, \end{aligned} \quad (7)$$

while the vertex corrections $\tilde{\sigma}_{\mu\nu,VC}^{(1)}$ are evaluated according to the original CPA theory²³ adapted to the TB-LMTO formalism³¹. The symbols $\bar{g}_\pm(E)$ in Eq. (7) and $\bar{g}(z)$ in the following text denote the configuration averages of $g_\pm(E)$ and $g(z)$, respectively. These quantities are given by $\bar{g}(z) = [\mathcal{P}(z) - S]^{-1}$, where $\mathcal{P}(z)$ is a site-diagonal matrix of the coherent potential functions. The treatment of the Fermi sea term (6) is done similarly to the case of the charge conductivity tensor²⁵; the details are given in Section II B.

B. Configuration averaging of the Fermi sea term

For the CPA-average of the Fermi sea term (6), we use the relation

$$\text{Tr} \langle \tilde{v}_\mu g'(z) v_\nu g(z) \rangle = \lim_{z_1 \rightarrow z} \frac{\partial}{\partial z_1} \text{Tr} \langle \tilde{v}_\mu g(z_1) v_\nu g(z) \rangle, \quad (8)$$

where the average on the r.h.s. can be split into the coherent part and the vertex corrections:

$$\text{Tr} \langle \tilde{v}_\mu g(z_1) v_\nu g(z) \rangle = \text{Tr} \{ \tilde{v}_\mu \bar{g}(z_1) v_\nu \bar{g}(z) \} + \text{Tr} \langle \tilde{v}_\mu g(z_1) v_\nu g(z) \rangle_{\text{VC}}. \quad (9)$$

The second term can be written according to the general expression³¹ as

$$\begin{aligned} \text{Tr} \langle \tilde{v}_\mu g(z_1) v_\nu g(z) \rangle_{\text{VC}} = \sum_{\mathbf{R}_1 \Lambda_1} \sum_{\mathbf{R}_2 \Lambda_2} & [\bar{g}(z) \tilde{v}_\mu \bar{g}(z_1)]_{\mathbf{R}_1 \mathbf{R}_1}^{L'_1 L_1} [\Delta^{-1}(z_1, z)]_{\mathbf{R}_1 \mathbf{R}_2}^{\Lambda_1 \Lambda_2} \\ & \times [\bar{g}(z_1) v_\nu \bar{g}(z)]_{\mathbf{R}_2 \mathbf{R}_2}^{L_2 L'_2}, \end{aligned} \quad (10)$$

where the symbols Λ_1 and Λ_2 abbreviate the composed orbital indices $\Lambda_1 = (L_1, L'_1)$ and $\Lambda_2 = (L_2, L'_2)$, respectively, and where the matrix $\Delta_{\mathbf{R}_1 \mathbf{R}_2}^{\Lambda_1 \Lambda_2}(z_1, z_2)$ was defined in the Appendix of Ref. 31. The evaluation of the vertex contribution to Eq. (8) is partly simplified due to the exact vanishing of the on-site blocks of the matrix product $\bar{g}(z)v_\nu\bar{g}(z)$:

$$[\bar{g}(z)v_\nu\bar{g}(z)]_{\mathbf{R}\mathbf{R}}^{LL'} = 0, \quad (11)$$

which is valid for the same energy arguments of both Green's functions. This rule is a consequence of a simple form of the coordinate operators X_μ and of the single-site nature of the coherent potential functions $\mathcal{P}(z)$, see Ref. 25 for details. After taking the partial derivative with respect to z_1 of Eq. (10), making the limit $z_1 \rightarrow z$, and using the rule (11), we get

$$\lim_{z_1 \rightarrow z} \frac{\partial}{\partial z_1} \text{Tr}\langle v_\mu g(z_1)v_\nu g(z)\rangle_{\text{VC}} = \sum_{\mathbf{R}_1 \Lambda_1} \sum_{\mathbf{R}_2 \Lambda_2} [\bar{g}\tilde{v}_\mu\bar{g}]_{\mathbf{R}_1 \mathbf{R}_1}^{L'_1 L_1} [\Delta^{-1}]_{\mathbf{R}_1 \mathbf{R}_2}^{\Lambda_1 \Lambda_2} [\bar{g}'v_\nu\bar{g}]_{\mathbf{R}_2 \mathbf{R}_2}^{L_2 L'_2}, \quad (12)$$

where all energy arguments on the r.h.s. (equal to z) were omitted for brevity. We can thus write the resulting average in Eq. (8) as

$$\text{Tr}\langle \tilde{v}_\mu g' v_\nu g \rangle = \text{Tr}\{\tilde{v}_\mu \bar{g}' v_\nu \bar{g}\} + \sum_{\mathbf{R}_1 \Lambda_1} \sum_{\mathbf{R}_2 \Lambda_2} [\bar{g}\tilde{v}_\mu\bar{g}]_{\mathbf{R}_1 \mathbf{R}_1}^{L'_1 L_1} [\Delta^{-1}]_{\mathbf{R}_1 \mathbf{R}_2}^{\Lambda_1 \Lambda_2} [\bar{g}'v_\nu\bar{g}]_{\mathbf{R}_2 \mathbf{R}_2}^{L_2 L'_2}, \quad (13)$$

and, similarly, one can derive the relation

$$\text{Tr}\langle \tilde{v}_\mu g v_\nu g' \rangle = \text{Tr}\{\tilde{v}_\mu \bar{g} v_\nu \bar{g}'\} + \sum_{\mathbf{R}_1 \Lambda_1} \sum_{\mathbf{R}_2 \Lambda_2} [\bar{g}\tilde{v}_\mu\bar{g}]_{\mathbf{R}_1 \mathbf{R}_1}^{L'_1 L_1} [\Delta^{-1}]_{\mathbf{R}_1 \mathbf{R}_2}^{\Lambda_1 \Lambda_2} [\bar{g}v_\nu\bar{g}']_{\mathbf{R}_2 \mathbf{R}_2}^{L_2 L'_2}. \quad (14)$$

Note that the second terms on the r.h.s. of (13) and (14) differ mutually only by their signs as a direct consequence of the rule (11).

The resulting coherent (coh) and vertex (VC) contributions to the Fermi sea term $\tilde{\sigma}_{\mu\nu}^{(2)} = \tilde{\sigma}_{\mu\nu, \text{coh}}^{(2)} + \tilde{\sigma}_{\mu\nu, \text{VC}}^{(2)}$ are given from the respective terms in (13) and (14):

$$\tilde{\sigma}_{\mu\nu, \text{coh}}^{(2)} = \sigma_0 \int_C dz \text{Tr}\{\tilde{v}_\mu \bar{g}'(z) v_\nu \bar{g}(z) - \tilde{v}_\mu \bar{g}(z) v_\nu \bar{g}'(z)\}, \quad (15)$$

and

$$\tilde{\sigma}_{\mu\nu, \text{VC}}^{(2)} = 2\sigma_0 \int_C dz \sum_{\mathbf{R}_1 \Lambda_1} \sum_{\mathbf{R}_2 \Lambda_2} [\bar{g}\tilde{v}_\mu\bar{g}]_{\mathbf{R}_1 \mathbf{R}_1}^{L'_1 L_1} [\Delta^{-1}]_{\mathbf{R}_1 \mathbf{R}_2}^{\Lambda_1 \Lambda_2} [\bar{g}'v_\nu\bar{g}]_{\mathbf{R}_2 \mathbf{R}_2}^{L_2 L'_2}, \quad (16)$$

where the energy argument z in $\bar{g}(z)$, $\bar{g}'(z)$ and $\Delta(z, z)$ has been suppressed for brevity. The appearance of the incoherent part of the Fermi sea term (16) represents the main difference between the spin-dependent and standard conductivity tensors in the TB-LMTO-CPA formalism, since the Fermi sea term in $\sigma_{\mu\nu}$ is purely coherent²⁵.

The energy derivative of the auxiliary Green's function, encountered in (15) and (16), is obtained from the rule $\bar{g}'(z) = -\bar{g}(z)\mathcal{P}'(z)\bar{g}(z)$, which follows from the energy independent structure constants S . As discussed in detail in Ref. 25, the formulation of the energy derivative $\mathcal{P}'(z)$ leads to CPA-vertex corrections involving an inversion of the same kernel $\Delta(z, z)$ as in $\tilde{\sigma}_{\mu\nu, \text{VC}}^{(2)}$ (16). This simplifies the numerical evaluation.

C. Transformation properties of the spin-dependent conductivity tensor

Since the enhanced numerical efficiency of the TB-LMTO method as compared to the original (canonical) LMTO technique is due to the screening of the structure constants, which depends on the chosen LMTO representation α ^{29,32}, the invariance of all physical quantities with respect to α is a necessary condition for any proper theoretical formalism. In the context of relativistic transport properties, this check has been done in detail for the standard conductivity tensor $\sigma_{\mu\nu}$ (1) in Ref. 25 and for the Gilbert damping tensor in Ref. 33.

In the case of the spin-dependent conductivity tensor $\tilde{\sigma}_{\mu\nu}$ (3) and of its Fermi surface and Fermi sea terms, the detailed study is outlined in Appendix A. Here we merely list the quantities invariant with respect to the choice of LMTO representation: (i) the total tensor $\tilde{\sigma}_{\mu\nu}$, (ii) the sum of the coherent contributions to the Fermi surface and Fermi sea terms, i.e., $\tilde{\sigma}_{\mu\nu, \text{coh}}^{(1)} + \tilde{\sigma}_{\mu\nu, \text{coh}}^{(2)}$, (iii) the vertex corrections to the Fermi surface term, $\tilde{\sigma}_{\mu\nu, \text{VC}}^{(1)}$, and (iv) the vertex corrections to the Fermi sea term, $\tilde{\sigma}_{\mu\nu, \text{VC}}^{(2)}$.

In analogy with the theory of the charge conductivity tensor²⁵, the above invariant contributions to the total spin-dependent conductivity tensor $\tilde{\sigma}_{\mu\nu}$ can be used for the definition of its intrinsic part, given by the sum of the coherent terms $\tilde{\sigma}_{\mu\nu,\text{coh}}^{(1)} + \tilde{\sigma}_{\mu\nu,\text{coh}}^{(2)}$, and of its extrinsic part, equal to the sum of the incoherent terms (vertex corrections) $\tilde{\sigma}_{\mu\nu,\text{VC}}^{(1)} + \tilde{\sigma}_{\mu\nu,\text{VC}}^{(2)}$. Since the tensor $\tilde{\sigma}_{\mu\nu}$ contains the SHC, this separation is naturally extended also to the intrinsic and extrinsic SHC. The extrinsic SHC is dominated by the Fermi surface contribution, which is due to the skew scattering and which diverges in the dilute limit, whereas the Fermi sea contribution is practically negligible both in diluted and concentrated alloys, see Section III. This classification is essentially identical to that adopted in previous *ab initio* theories of the SHE^{7,8,11}.

D. Implementation and numerical details

The numerical implementation of the developed formalism and the performed calculations follow closely our recent works focused on the Fermi surface²⁴ and Fermi sea²⁵ terms of the charge conductivity tensor. We have employed the *spd*-basis of the selfconsistent relativistic TB-LMTO-CPA method³⁴, added a small imaginary part of $\pm 10^{-5}$ Ry to the Fermi energy E_F in evaluation of $\tilde{\sigma}_{\mu\nu}^{(1)}$, and used 20 – 40 complex nodes for integrations along the complex contour C in evaluation of $\tilde{\sigma}_{\mu\nu}^{(2)}$. The Brillouin zone integrals were performed with sufficient numbers of \mathbf{k} points; for the complex energy arguments closest to the real Fermi energy, total numbers of $\sim 10^8$ sampling points were used.

III. RESULTS AND DISCUSSION

The first results of the developed theory, discussed in this paper, refer to nonmagnetic random binary alloys on fcc lattices. As a consequence of the full cubic symmetry and time-inversion symmetry¹⁴, the only independent nonzero element of the tensor $\sigma_{\mu\nu}^\lambda$ (2) is σ_{xy}^z which is equivalent to $\tilde{\sigma}_{xy}$ (3) with the spin-polarization vector \mathbf{n} along z axis. This element is identified with the SHC in the following.

A. Random alloy in a tight-binding *sp*-model

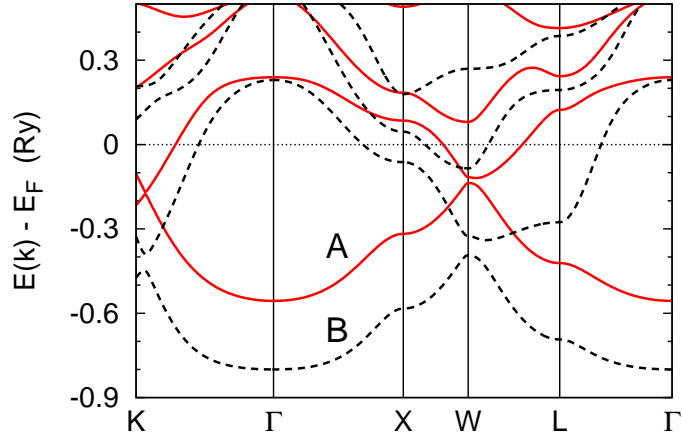


FIG. 1. Band structures of pure metals A (full lines) and B (dashed lines) in a tight-binding *sp*-model on fcc lattice. The horizontal dotted line denotes the position of the Fermi energy.

In order to investigate the behavior of the three contributions to the SHC (Section II C) in a dilute limit, we have studied a simple tight-binding model of a random binary alloy $A_{1-c}B_c$ on an fcc lattice. The model assumes *sp*-orbitals on each lattice site with a site-diagonal disorder present in the LMTO potential parameters of both alloy constituents; the band structures of ideal fcc metals A and B are displayed in Fig. 1. The species A is lighter than the species B, which is reflected by higher eigenvalues of A as compared to those of B. Note that only one band (including its double degeneracy) intersects the Fermi energy for metal A, whereas two bands cross the E_F for metal B. Simultaneously,

the strength of spin-orbit coupling of A is smaller than that of B which is documented, e.g., by a smaller splitting of the two lowest bands of A at the point W as compared to the corresponding splitting of B.

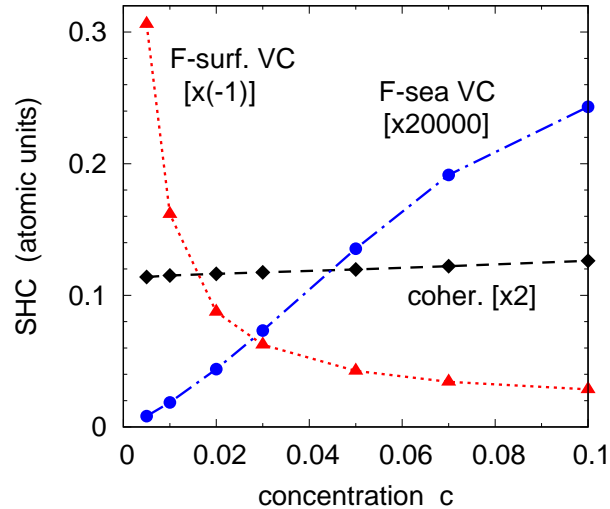


FIG. 2. Three contributions to the spin Hall conductivity (SHC) for a tight-binding sp -model of a random fcc alloy $A_{1-c}B_c$ as functions of the concentration c : the coherent term (diamonds), the vertex corrections to the Fermi surface term (triangles), and the vertex corrections to the Fermi sea term (circles). These contributions were rescaled by a factor of 2, -1 , and 20000 , respectively.

In this simple model of a random $A_{1-c}B_c$ alloy, the fcc lattice parameter, the species-resolved LMTO potential parameters, and the alloy Fermi energy were kept fixed (independent on the concentration c). The resulting SHC-contributions in the dilute alloy for $c \rightarrow 0$ are shown in Fig. 2; the SHC values are given in atomic units which is sufficient for the present purpose. One can see that the three contributions exhibit three different concentration trends for the vanishing impurity content: the coherent term ($\tilde{\sigma}_{xy,coh}^{(1)} + \tilde{\sigma}_{xy,coh}^{(2)}$) exhibits a finite nonzero limit, the Fermi surface vertex term ($\tilde{\sigma}_{xy,VC}^{(1)}$) diverges with an inverse proportionality to c , and the Fermi sea vertex term ($\tilde{\sigma}_{xy,VC}^{(2)}$) vanishes roughly linearly with c .

The divergence of the Fermi surface vertex term has been obtained and discussed by a number of authors^{3,7,8}; this behavior of the extrinsic SHC has been ascribed to skew scattering. The weakly concentration dependent coherent term has also been found earlier^{8,11}. This trend justifies an identification of the coherent term with the intrinsic SHC of random alloys. Let us note however that the limit of the coherent SHC term for $c \rightarrow 0$ does not necessarily coincide with the SHC of the pure host metal A evaluated by using the Berry curvature approach from its band structure. This fact can probably be explained by a sensitivity of the alloy selfenergy to the impurity B potential which contributes to the limiting value of the intrinsic SHC for $c \rightarrow 0$. A complete analysis of this point goes beyond the scope of this work.

The vertex corrections to the Fermi sea term have not been explicitly studied by other authors in the dilute limit. Since the same kernel $\Delta(z, z)$ is inverted in evaluation of Eq. (16) and in obtaining the energy derivative of the coherent potential function $\mathcal{P}'(z)$, the revealed proportionality $\tilde{\sigma}_{xy,VC}^{(2)} \sim c$ can be understood as a counterpart of the limiting behavior $\mathcal{P}'(z) \rightarrow P_A'(z)$ for $c \rightarrow 0$, where $P_A(z)$ denotes the potential function of the host metal A. Note however the very small magnitude of the incoherent Fermi sea term as compared to the other two terms (Fig. 2); since similarly tiny magnitudes were found for realistic alloy models even in concentrated regimes (Section III B), a more detailed discussion of this term seems to be of little importance.

B. Random fcc Pt-based alloys

In this section, we address random fcc alloys of Pt with other heavy metals Au, Re, and Ta. For all systems, the average Wigner-Seitz (atomic sphere) radius of the alloy was set according to the Vegard's law and the experimental values of the atomic sphere radii of the pure elements in their equilibrium structures. Local lattice relaxations were ignored which is acceptable because of similar sizes of all four elements.

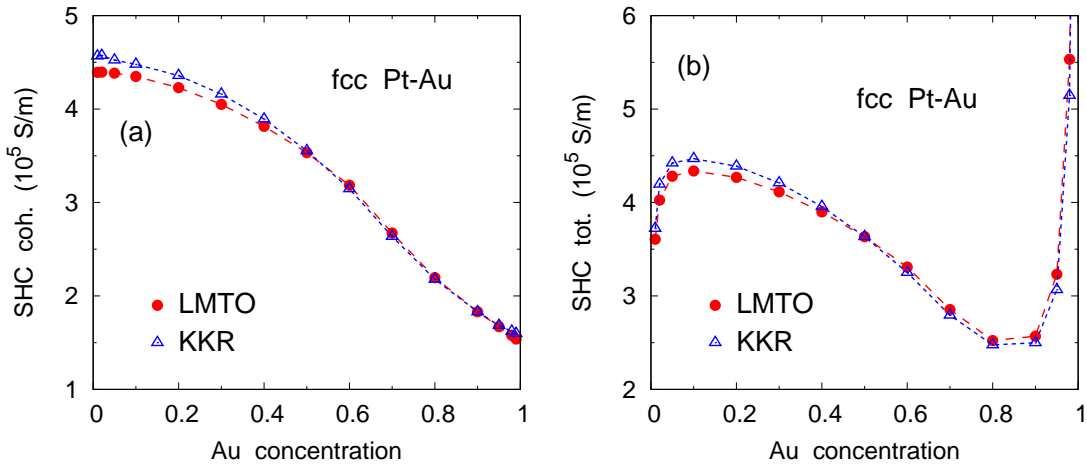


FIG. 3. Comparison of the spin Hall conductivities (SHC) calculated in the TB-LMTO (solid circles) and KKR (open triangles) techniques for random fcc Pt-Au alloys: (a) the coherent part of the SHC, and (b) the total SHC, both as functions of Au concentration. The results of the KKR method were taken from Ref. 12.

The total SHC and its intrinsic part for Pt-Au alloys are shown in Fig. 3; the TB-LMTO results are compared with those of the relativistic Korring-Kohn-Rostoker (KKR) method¹². One can see a very good agreement between both methods taking into account the different spin-current operators used: random, site-diagonal operators enter the KKR technique¹⁶, whereas nonrandom, non-site-diagonal effective operators are employed in the present work (Section II A). The intrinsic SHC decreases monotonically with increasing Au concentration (Fig. 3a); the extrinsic contribution modifies this trend significantly only near the limits of pure Pt and pure Au (Fig. 3b), where the divergent behavior dominates. For all concentrations, the vertex corrections to the Fermi sea term are about four orders of magnitude smaller than the SHC values in Fig. 3 and can thus be safely ignored. This feature has also been found in the KKR results³⁵.

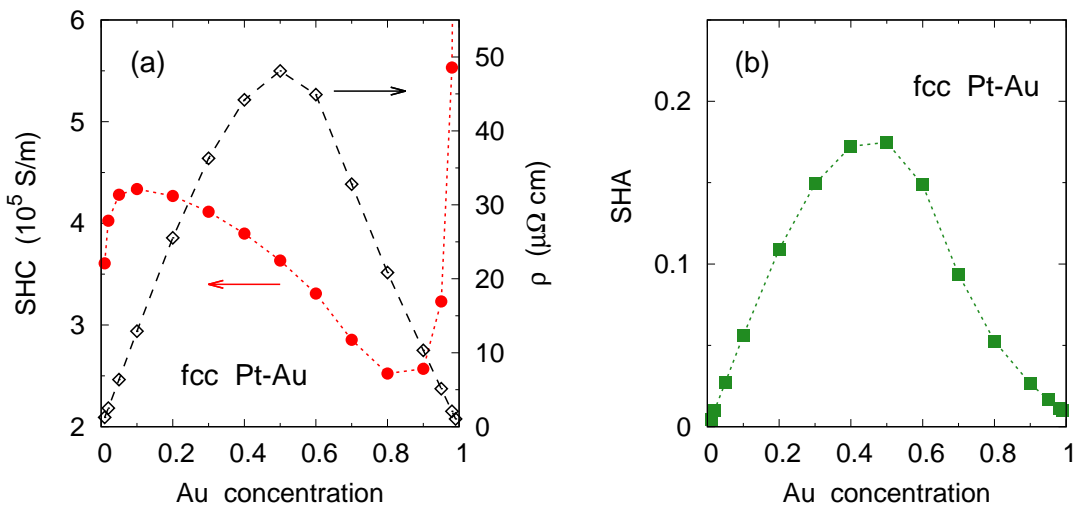


FIG. 4. The calculated spin Hall conductivities (SHC), residual resistivities (ρ), and spin Hall angles (SHA) in random fcc Pt-Au alloys as functions of Au concentration: (a) SHC (solid circles, left scale) and ρ (open diamonds, right scale), and (b) SHA (solid squares).

The calculated SHC values compare reasonably well to the measured ones in the entire concentration interval¹². Figure 4 displays the concentration trend of the SHC and of other transport quantities: the longitudinal resistivity ρ and the SHA given by the product $\tilde{\sigma}_{xy}\rho$. One can see a maximum of ρ for the equiconcentration alloy (Fig. 4a); a very similar concentration trend is obtained for the SHA with a maximum value slightly below 0.2 (Fig. 4b) which agrees

again with the KKR results¹². This value is comparable with the top SHA values obtained for other alloys based on 5d transition metals^{12,36}. Note however that the equiconcentration Pt-Au system is not thermodynamically stable at ambient temperatures according to its equilibrium phase diagram³⁷ so that the measured samples are stabilized only by kinetic barriers. This fact calls for inspection of other alloy systems which might exhibit sizeable SHA values for substitutional solid solutions that are equilibrium phases at low temperatures.

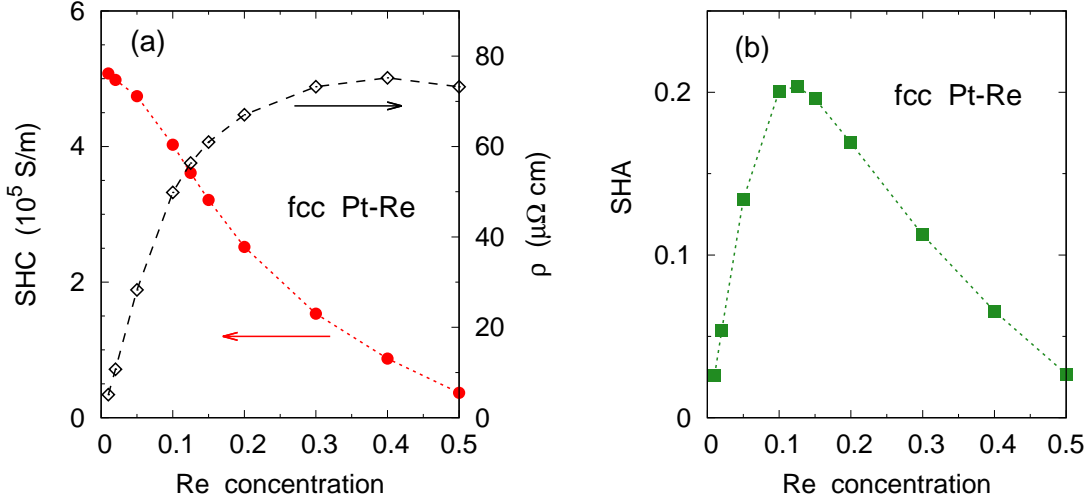


FIG. 5. The same as Fig. 4, but for random fcc Pt-Re alloys.

In this work, we confined our interest to Pt-based alloys with fcc structure. The solubility limit of Re in fcc Pt is about 40 at.% Re³⁷. The calculated values of SHC, ρ , and SHA are shown in Fig. 5. One can see a decreasing trend of the SHC due to alloying by Re, which is accompanied by a steep increase of the resistivity ρ for small Re contents followed by a saturation of ρ for higher Re concentrations (Fig. 5a). As a result of these trends, the SHA exhibits a maximum value of about 0.2 for Re content around 12 at.% Re (Fig. 5b). This composition falls safely inside the solubility interval of this alloy system and the predicted SHA value thus might deserve future experimental verification.

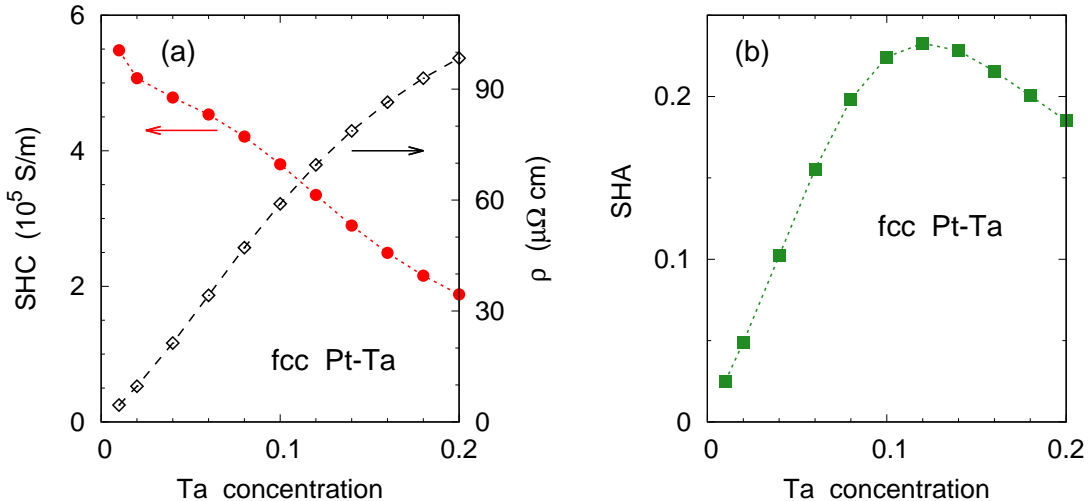


FIG. 6. The same as Fig. 4, but for random fcc Pt-Ta alloys.

The phase diagram of Pt-rich Pt-Ta system at ambient temperatures is not exactly known at present; extrapolations from higher temperatures indicate that the low-temperature solubility limit is about 15 at.% Ta³⁷. The relevant collection of calculated SHC, ρ , and SHA is displayed in Fig. 6. One can observe opposite trends of SHC and ρ due

to alloying by Ta (Fig. 6a), in analogy with the Pt-Au (Fig. 4a) and Pt-Re (Fig. 5a) systems. The SHA exhibits a maximum again; the maximum SHA exceeds slightly the value 0.2 which is obtained for the alloy with about 12 at.% Ta (Fig. 6b). This composition should correspond to a thermodynamically stable primary solid solution.

The obtained maximum SHA values in all three studied Pt-based alloys result from a delicate competition between a reduction of SHC and an increase of ρ due to alloying. Since these maximum values increase in sequence Pt-Au, Pt-Re, and Pt-Ta, one can ascribe a more important role to variations of ρ which increases in the same sequence, as can be seen, e.g., by comparing the resistivities for alloys with 20 at.% of impurities. This importance of the longitudinal resistivity for large SHA values is in line with recent findings for the SHE in amorphous Hf-W alloys³⁶ as well as for SHE-based spin torques in multilayers with Pt-Al and Pt-Hf alloys³⁸. Moreover, the resistivity variation is also responsible for the temperature dependence of the SHA both in bulk Pt-Au alloys¹² and in Pt layers adjacent to ferromagnetic Ni-Fe alloys¹³.

IV. CONCLUSIONS

We have modified our recent theory of the relativistic electron transport in random alloys within the TB-LMTO-CPA method²⁵ for the spin-dependent conductivity tensor. The derived formalism leads in general to three contributions to this tensor, namely, (i) a coherent part, (ii) an incoherent part of the Fermi surface term, and (iii) an incoherent part of the Fermi sea term, which are all invariant with respect to the chosen TB-LMTO representation. The coherent part can be identified with an intrinsic contribution to the tensor, whereas the incoherent parts lead to an extrinsic contribution.

The developed theory is in principle applicable to a wide spectrum of phenomena involving spin-polarized currents induced by external electric fields encountered in systems with or without spontaneous magnetic moments. The performed analysis and calculations related to the spin Hall effect in nonmagnetic alloys revealed that the three contributions to the spin Hall conductivity exhibit three different concentration trends in the dilute limit and that the incoherent part of the Fermi sea term is negligibly small in the entire concentration interval. The obtained results for selected Pt-based binary alloys indicate that sizeable values of the spin Hall angles can be obtained even for thermodynamically equilibrium primary solid solutions as an alternative to often studied metastable crystalline and amorphous alloys.

The approach worked out in this paper is not restricted only to the spin currents as observables; the derived formulas for the spin-dependent conductivity tensor represent essentially a complete result (within the TB-LMTO-CPA method) for the static linear response of any quantity to an external electric field. For this reason, a possible extension of the present theory towards a treatment of spin-orbit torques due to electric fields³⁹⁻⁴¹ seems (with the use of nonrandom effective torque operators³³) quite promising.

ACKNOWLEDGMENTS

The authors acknowledge financial support from the Czech Science Foundation (Grant No. 18-07172S).

Appendix A: Transformation invariance of the spin-dependent conductivity tensor

1. One-particle quantities

The study of the invariance of physical quantities with respect to the choice of the LMTO representation is based on relations for the coherent potential functions and the structure constants in two different representations, denoted by superscripts α and β :

$$\mathcal{P}^\alpha(z) = [1 + \mathcal{P}^\beta(z)(\beta - \alpha)]^{-1} \mathcal{P}^\beta(z), \quad S^\alpha = [1 + S^\beta(\beta - \alpha)]^{-1} S^\beta, \quad (A1)$$

where the quantities α and β in the brackets denote non-random site-diagonal matrices of the screening constants.^{32,34} Let us introduce $\eta = \beta - \alpha$ and

$$\begin{aligned} M(z) &= 1 + \mathcal{P}^\beta(z)\eta, & M^\times(z) &= 1 + \eta\mathcal{P}^\beta(z), \\ K &= 1 + S^\beta\eta, & K^\times &= 1 + \eta S^\beta, \end{aligned} \quad (A2)$$

and let us abbreviate $\bar{g}_\pm = \lim_{\epsilon \rightarrow 0^+} \bar{g}(E_F \pm i\epsilon)$ [and similarly for other energy dependent quantities, such as the coherent potential functions $\mathcal{P}(z)$, the site-diagonal matrices $M(z)$ and $M^\times(z)$, and the single-site T-matrices $t_{\mathbf{R}}(z)$]. The transformation properties of the average auxiliary Green's function $\bar{g}(z)$ can be summarized as

$$\begin{aligned}\bar{g}^\alpha(z) &= M^\times(z)\bar{g}^\beta(z)M(z) - \eta M(z) = K^\times\bar{g}^\beta(z)K + K^\times\eta \\ &= M^\times(z)\bar{g}^\beta(z)K = K^\times\bar{g}^\beta(z)M(z),\end{aligned}\quad (\text{A3})$$

the energy derivative of $\bar{g}(z)$ transforms as

$$\bar{g}'^{\alpha}(z) = K^\times [\bar{g}'^{\beta}(z)M(z) + \bar{g}^\beta(z)M'(z)] = K^\times\bar{g}'^{\beta}(z)K, \quad (\text{A4})$$

and the transformation rule for the difference of two Green's functions is

$$\bar{g}_+^\alpha - \bar{g}_-^\alpha = K^\times(\bar{g}_+^\beta - \bar{g}_-^\beta)K. \quad (\text{A5})$$

The transformation properties of the effective velocities \tilde{v}_μ and v_ν are given by

$$\tilde{v}_\mu^\alpha = K^{-1}\tilde{v}_\mu^\beta(K^\times)^{-1}, \quad v_\nu^\alpha = K^{-1}v_\nu^\beta(K^\times)^{-1}. \quad (\text{A6})$$

All these transformation rules can be proved by procedures similar to those found in Ref. 24 and 32, taking into account also the spin-independence of matrices $\alpha, \beta, S^\alpha, S^\beta$, and K .

The on-site blocks $M_{\mathbf{R}}(z)$ and $M_{\mathbf{R}}^\times(z)$ of the respective site-diagonal matrices $M(z)$ and $M^\times(z)$ enter also the transformation of the LMTO-CPA single-site T-matrices $t_{\mathbf{R}}(z)$, namely,

$$t_{\mathbf{R}}^\beta(z) = M_{\mathbf{R}}(z)t_{\mathbf{R}}^\alpha(z)M_{\mathbf{R}}^\times(z), \quad (\text{A7})$$

see Refs. 34 and 42 for more details.

2. Coherent contributions

The transformation of the coherent part of the Fermi surface term (5) is

$$\tilde{\sigma}_{\mu\nu,\text{coh}}^{(1),\alpha} = \sigma_0 \text{Tr} \{ \tilde{v}_\mu^\alpha(\bar{g}_+^\alpha - \bar{g}_-^\alpha)v_\nu^\alpha\bar{g}_-^\alpha - \tilde{v}_\mu^\alpha\bar{g}_+^\alpha v_\nu^\alpha(\bar{g}_+^\alpha - \bar{g}_-^\alpha) \} = \tilde{\sigma}_{\mu\nu,\text{coh}}^{(1),\beta} + Z_{\mu\nu}, \quad (\text{A8})$$

where the remainder can be written as

$$\begin{aligned}Z_{\mu\nu} &= \sigma_0 \text{Tr} \{ \tilde{v}_\mu^\beta(\bar{g}_+^\beta - \bar{g}_-^\beta)v_\nu^\beta\eta K^{-1} - \tilde{v}_\mu^\beta\eta K^{-1}v_\nu^\beta(\bar{g}_+^\beta - \bar{g}_-^\beta) \} \\ &= \sigma_0 \text{Tr} \{ Y_{\mu\nu}(\bar{g}_+^\beta - \bar{g}_-^\beta) \}, \quad Y_{\mu\nu} = v_\nu^\beta\eta K^{-1}\tilde{v}_\mu^\beta - \tilde{v}_\mu^\beta\eta K^{-1}v_\nu^\beta.\end{aligned}\quad (\text{A9})$$

This result proves that for metallic systems, the coherent part of $\tilde{\sigma}_{\mu\nu}^{(1)}$ depends on the particular LMTO representation.

The coherent part of the Fermi sea term (15) transforms as

$$\tilde{\sigma}_{\mu\nu,\text{coh}}^{(2),\alpha} = \sigma_0 \int_C dz \text{Tr} \{ \tilde{v}_\mu^\alpha\bar{g}'^{\alpha}(z)v_\nu^\alpha\bar{g}^\alpha(z) - \tilde{v}_\mu^\alpha\bar{g}^\alpha(z)v_\nu^\alpha\bar{g}'^{\alpha}(z) \} = \tilde{\sigma}_{\mu\nu,\text{coh}}^{(2),\beta} + R_{\mu\nu}, \quad (\text{A10})$$

where the remainder is

$$R_{\mu\nu} = \sigma_0 \int_C dz \text{Tr} \{ \tilde{v}_\mu^\beta\bar{g}'^{\beta}(z)v_\nu^\beta\eta K^{-1} - \tilde{v}_\mu^\beta\eta K^{-1}v_\nu^\beta\bar{g}'^{\beta}(z) \}. \quad (\text{A11})$$

This remainder can be rewritten with the use of $\int_C dz \bar{g}'^{\beta}(z) = \bar{g}_-^\beta - \bar{g}_+^\beta$, which yields

$$R_{\mu\nu} = \sigma_0 \text{Tr} \{ Y_{\mu\nu}(\bar{g}_-^\beta - \bar{g}_+^\beta) \} = -Z_{\mu\nu}. \quad (\text{A12})$$

This result proves that the coherent part of $\tilde{\sigma}_{\mu\nu}^{(2)}$ depends on the choice of the LMTO representation as well, but the sum $\tilde{\sigma}_{\mu\nu,\text{coh}}^{(1)} + \tilde{\sigma}_{\mu\nu,\text{coh}}^{(2)}$, i.e., the total coherent part of $\tilde{\sigma}_{\mu\nu}$, is strictly invariant, as mentioned in Section II C.

3. Incoherent part of the Fermi surface term

For the vertex corrections to the Fermi surface term (5), transformation properties are needed for all quantities entering the general expression for the LMTO vertex corrections³¹, see also Eq. (10). The transformation rule for a two-particle quantity $\chi_{\mathbf{R}_1 \mathbf{R}_2}^{\Lambda_1 \Lambda_2}$ depending only on elements of the average auxiliary Green's functions between different sites ($\mathbf{R}_1 \neq \mathbf{R}_2$) and defined as

$$\chi_{\mathbf{R}_1 \mathbf{R}_2}^{\Lambda_1 \Lambda_2} = (1 - \delta_{\mathbf{R}_1 \mathbf{R}_2})(\bar{g}_+)^{L_1 L_2}_{\mathbf{R}_1 \mathbf{R}_2} (\bar{g}_-)^{L'_1 L'_2}_{\mathbf{R}_2 \mathbf{R}_1}, \quad (\text{A13})$$

where $\Lambda_1 = (L_1, L'_1)$, $\Lambda_2 = (L_2, L'_2)$, is given with help of Eq. (A3) by

$$\chi^\alpha = \Pi \chi^\beta \tilde{\Pi}, \quad (\text{A14})$$

where we introduced site-diagonal quantities $\Pi_{\mathbf{R}_1 \mathbf{R}_2}^{\Lambda_1 \Lambda_2} = \delta_{\mathbf{R}_1 \mathbf{R}_2} \Pi_{\mathbf{R}_1}^{\Lambda_1 \Lambda_2}$ and $\tilde{\Pi}_{\mathbf{R}_1 \mathbf{R}_2}^{\Lambda_1 \Lambda_2} = \delta_{\mathbf{R}_1 \mathbf{R}_2} \tilde{\Pi}_{\mathbf{R}_1}^{\Lambda_1 \Lambda_2}$, where

$$\Pi_{\mathbf{R}}^{\Lambda_1 \Lambda_2} = \left(M_{+, \mathbf{R}}^\times \right)^{L_1 L_2} (M_{-, \mathbf{R}})^{L'_2 L'_1}, \quad \tilde{\Pi}_{\mathbf{R}}^{\Lambda_1 \Lambda_2} = (M_{+, \mathbf{R}})^{L_1 L_2} \left(M_{-, \mathbf{R}}^\times \right)^{L'_2 L'_1}. \quad (\text{A15})$$

The site-diagonal quantity $w_{\mathbf{R}_1 \mathbf{R}_2}^{\Lambda_1 \Lambda_2} = \delta_{\mathbf{R}_1 \mathbf{R}_2} w_{\mathbf{R}_1}^{\Lambda_1 \Lambda_2}$, where $w_{\mathbf{R}}^{\Lambda_1 \Lambda_2} = \langle t_{+, \mathbf{R}}^{L_1 L_2} t_{-, \mathbf{R}}^{L'_2 L'_1} \rangle$, satisfies the transformation relation

$$w^\beta = \tilde{\Pi} w^\alpha \Pi, \quad (\text{A16})$$

which follows from Eq. (A7). As a consequence of the rules (A14) and (A16), the matrix $\Delta = w^{-1} - \chi$ and its inverse transform as

$$\Delta^\alpha = \Pi \Delta^\beta \tilde{\Pi}, \quad (\Delta^\alpha)^{-1} = \tilde{\Pi}^{-1} (\Delta^\beta)^{-1} \Pi^{-1}. \quad (\text{A17})$$

For transformations of the on-site blocks $(\bar{g}_+ v_\nu \bar{g}_-)_{\mathbf{R} \mathbf{R}}^{L_1 L'_1} \equiv (\bar{g}_+ v_\nu \bar{g}_-)_{\mathbf{R}}^{\Lambda_1}$ and $(\bar{g}_- \tilde{v}_\mu \bar{g}_+)_{\mathbf{R} \mathbf{R}}^{L'_1 L_1} \equiv (\bar{g}_- \tilde{v}_\mu \bar{g}_+)_{\mathbf{R}}^{\tilde{\Lambda}_1}$, one can use relations (A3) and (A6) for the Green's functions and velocities, respectively. The result is

$$(\bar{g}_+^\alpha v_\nu^\alpha \bar{g}_-^\alpha)_{\mathbf{R}}^{\Lambda_1} = \sum_{\Lambda_2} \Pi_{\mathbf{R}}^{\Lambda_1 \Lambda_2} (\bar{g}_+^\beta v_\nu^\beta \bar{g}_-^\beta)_{\mathbf{R}}^{\Lambda_2}, \quad (\bar{g}_-^\alpha \tilde{v}_\mu^\alpha \bar{g}_+^\alpha)_{\mathbf{R}}^{\tilde{\Lambda}_1} = \sum_{\Lambda_2} (\bar{g}_-^\beta \tilde{v}_\mu^\beta \bar{g}_+^\beta)_{\mathbf{R}}^{\tilde{\Lambda}_2} \tilde{\Pi}_{\mathbf{R}}^{\Lambda_2 \Lambda_1}, \quad (\text{A18})$$

where the symbols $\tilde{\Lambda}_1 = (L'_1, L_1)$ and $\tilde{\Lambda}_2 = (L'_2, L_2)$ denote indices transposed to $\Lambda_1 = (L_1, L'_1)$ and $\Lambda_2 = (L_2, L'_2)$, respectively.

The calculation of the vertex part of the Fermi surface term (5) rests on the formula (10). The identity (11) yields $\text{Tr} \langle \tilde{v}_\mu g_+ v_\nu g_+ \rangle_{\text{VC}} = \text{Tr} \langle \tilde{v}_\mu g_- v_\nu g_- \rangle_{\text{VC}} = 0$, so that $\tilde{\sigma}_{\mu\nu, \text{VC}}^{(1)} = 2\sigma_0 \text{Tr} \langle \tilde{v}_\mu g_+ v_\nu g_- \rangle_{\text{VC}}$ and

$$\tilde{\sigma}_{\mu\nu, \text{VC}}^{(1), \alpha} = 2\sigma_0 \sum_{\mathbf{R}_1 \Lambda_1} \sum_{\mathbf{R}_2 \Lambda_2} (\bar{g}_-^\alpha \tilde{v}_\mu^\alpha \bar{g}_+^\alpha)_{\mathbf{R}_1}^{\tilde{\Lambda}_1} [(\Delta^\alpha)^{-1}]_{\mathbf{R}_1 \mathbf{R}_2}^{\Lambda_1 \Lambda_2} (\bar{g}_+^\alpha v_\nu^\alpha \bar{g}_-^\alpha)_{\mathbf{R}_2}^{\Lambda_2}. \quad (\text{A19})$$

The last relation combined with the transformations (A17) and (A18) leads to the invariance of the vertex corrections to the Fermi surface term, $\tilde{\sigma}_{\mu\nu, \text{VC}}^{(1), \alpha} = \tilde{\sigma}_{\mu\nu, \text{VC}}^{(1), \beta}$.

4. Incoherent part of the Fermi sea term

The vertex corrections to the Fermi sea term (16) can be written as $(-2\sigma_0) \int_C dz Q(z)$, where the quantity $Q(z)$ in the LMTO representation α is given explicitly by

$$Q^\alpha = \sum_{\mathbf{R}_1 \Lambda_1} \sum_{\mathbf{R}_2 \Lambda_2} (\bar{g}^\alpha \tilde{v}_\mu^\alpha \bar{g}^\alpha)_{\mathbf{R}_1}^{\tilde{\Lambda}_1} [(\Delta^\alpha)^{-1}]_{\mathbf{R}_1 \mathbf{R}_2}^{\Lambda_1 \Lambda_2} (\bar{g}^\alpha v_\nu^\alpha \bar{g}'^{\alpha})_{\mathbf{R}_2}^{\Lambda_2}, \quad (\text{A20})$$

where all energy arguments (equal to z) have been omitted, see Eq. (16), where $\Lambda_1 = (L_1, L'_1)$, $\Lambda_2 = (L_2, L'_2)$, $\tilde{\Lambda}_1 = (L'_1, L_1)$, and $\tilde{\Lambda}_2 = (L'_2, L_2)$, and where the same identifications have been done as before, namely, $(\bar{g} v_\nu \bar{g}')_{\mathbf{R} \mathbf{R}}^{L_1 L'_1} \equiv (\bar{g} v_\nu \bar{g}')_{\mathbf{R}}^{\Lambda_1}$ and $(\bar{g} \tilde{v}_\mu \bar{g})_{\mathbf{R} \mathbf{R}}^{L'_1 L_1} \equiv (\bar{g} \tilde{v}_\mu \bar{g})_{\mathbf{R}}^{\tilde{\Lambda}_1}$.

The transformation of individual factors in Eq. (A20) is similar to the previous case of the Fermi surface term. In particular, the transformation rules for Δ^α and its inverse, Eq. (A17), remain valid but with the quantities $\Pi_{\mathbf{R}}$ and $\tilde{\Pi}_{\mathbf{R}}$ defined as

$$\Pi_{\mathbf{R}}^{\Lambda_1 \Lambda_2} = (M_{\mathbf{R}}^\times)^{L_1 L_2} (M_{\mathbf{R}})^{L'_2 L'_1}, \quad \tilde{\Pi}_{\mathbf{R}}^{\Lambda_1 \Lambda_2} = (M_{\mathbf{R}})^{L_1 L_2} (M_{\mathbf{R}}^\times)^{L'_2 L'_1}, \quad (\text{A21})$$

where the matrices $M_{\mathbf{R}}$ and $M_{\mathbf{R}}^\times$ are taken with the same (omitted) energy argument z . The transformation of $(\bar{g} \tilde{v}_\mu \bar{g})_{\mathbf{R}}^{\tilde{\Lambda}_1}$ is similar to Eq. (A18), namely,

$$(\bar{g}^\alpha \tilde{v}_\mu^\alpha \bar{g}^\alpha)_{\mathbf{R}}^{\tilde{\Lambda}_1} = \sum_{\Lambda_2} (\bar{g}^\beta \tilde{v}_\mu^\beta \bar{g}^\beta)_{\mathbf{R}}^{\tilde{\Lambda}_2} \tilde{\Pi}_{\mathbf{R}}^{\Lambda_2 \Lambda_1}, \quad (\text{A22})$$

while the transformation of $(\bar{g} v_\nu \bar{g}')_{\mathbf{R}}^{\Lambda_1}$ is based on relation (A4), which leads to

$$(\bar{g}^\alpha v_\nu^\alpha \bar{g}'^\alpha)_{\mathbf{R}}^{L_1 L'_1} = (M^\times \bar{g}^\beta v_\nu^\beta \bar{g}'^\beta M)_{\mathbf{R}}^{L_1 L'_1} + (M^\times \bar{g}^\beta v_\nu^\beta \bar{g}^\beta M')_{\mathbf{R}}^{L_1 L'_1}, \quad (\text{A23})$$

where the second term on the r.h.s. vanishes due to the identity (11) and due to the site-diagonal nature of matrices M , M^\times and M' . This yields

$$(\bar{g}^\alpha v_\nu^\alpha \bar{g}'^\alpha)_{\mathbf{R}}^{\Lambda_1} = \sum_{\Lambda_2} \Pi_{\mathbf{R}}^{\Lambda_1 \Lambda_2} (\bar{g}^\beta v_\nu^\beta \bar{g}'^\beta)_{\mathbf{R}}^{\Lambda_2}, \quad (\text{A24})$$

again in analogy with Eq. (A18). The use of the rules (A17), (A22) and (A24) in Eq. (A20) leads to $Q^\alpha(z) = Q^\beta(z)$, which proves the transformation invariance of the vertex corrections to the Fermi sea term, $\tilde{\sigma}_{\mu\nu, \text{VC}}^{(2), \alpha} = \tilde{\sigma}_{\mu\nu, \text{VC}}^{(2), \beta}$.

This completes the proof of the invariance of the total spin-dependent conductivity tensor $\tilde{\sigma}_{\mu\nu}$ (4) with respect to the choice of the LMTO representation.

* turek@ipm.cz

† kudrnov@fzu.cz

‡ drchal@fzu.cz

- ¹ S. Maekawa, S. O. Valenzuela, E. Saitoh, and T. Kimura, eds., *Spin Current* (Oxford University Press, 2012).
- ² E. Y. Tsymbal and I. Žutić, eds., *Handbook of Spin Transport and Magnetism* (CRC Press, Boca Raton, 2012).
- ³ J. Sinova, S. O. Valenzuela, J. Wunderlich, C. H. Back, and T. Jungwirth, Rev. Mod. Phys. **87**, 1213 (2015).
- ⁴ J. E. Hirsch, Phys. Rev. Lett. **83**, 1834 (1999).
- ⁵ G. Y. Guo, S. Murakami, T.-W. Chen, and N. Nagaosa, Phys. Rev. Lett. **100**, 096401 (2008).
- ⁶ F. Freimuth, S. Blügel, and Y. Mokrousov, Phys. Rev. Lett. **105**, 246602 (2010).
- ⁷ M. Gradhand, D. V. Fedorov, P. Zahn, and I. Mertig, Phys. Rev. Lett. **104**, 186403 (2010).
- ⁸ S. Lowitzer, M. Gradhand, D. Ködderitzsch, D. V. Fedorov, I. Mertig, and H. Ebert, Phys. Rev. Lett. **106**, 056601 (2011).
- ⁹ N. Nagaosa, J. Sinova, S. Onoda, A. H. MacDonald, and N. P. Ong, Rev. Mod. Phys. **82**, 1539 (2010).
- ¹⁰ B. Zimmermann, K. Chadova, D. Ködderitzsch, S. Blügel, H. Ebert, D. V. Fedorov, N. H. Long, P. Mavropoulos, I. Mertig, Y. Mokrousov, and M. Gradhand, Phys. Rev. B **90**, 220403(R) (2014).
- ¹¹ K. Chadova, S. Wimmer, H. Ebert, and D. Ködderitzsch, Phys. Rev. B **92**, 235142 (2015).
- ¹² M. Obstbaum, M. Decker, A. K. Greitner, M. Haertinger, T. N. G. Meier, M. Kronseder, K. Chadova, S. Wimmer, D. Ködderitzsch, H. Ebert, and C. H. Back, Phys. Rev. Lett. **117**, 167204 (2016).
- ¹³ L. Wang, R. J. H. Wesseling, Y. Liu, Z. Yuan, K. Xia, and P. J. Kelly, Phys. Rev. Lett. **116**, 196602 (2016).
- ¹⁴ S. Wimmer, M. Seemann, K. Chadova, D. Ködderitzsch, and H. Ebert, Phys. Rev. B **92**, 041101(R) (2015).
- ¹⁵ D. C. Ralph and M. D. Stiles, J. Magn. Magn. Mater. **320**, 1190 (2008).
- ¹⁶ S. Lowitzer, D. Ködderitzsch, and H. Ebert, Phys. Rev. B **82**, 140402(R) (2010).
- ¹⁷ Y. Zhang, Y. Sun, H. Yang, J. Železný, S. P. P. Parkin, C. Felser, and B. Yan, Phys. Rev. B **95**, 075128 (2017).
- ¹⁸ Y. Zhang, J. Železný, Y. Sun, J. van den Brink, and B. Yan, New J. Phys. **20**, 073028 (2018).
- ¹⁹ Y. Wang, K. Xia, Z.-B. Su, and Z. Ma, Phys. Rev. Lett. **96**, 066601 (2006).
- ²⁰ J. Shi, P. Zhang, D. Xiao, and Q. Niu, Phys. Rev. Lett. **96**, 076604 (2006).
- ²¹ I. Turek, J. Kudrnovský, V. Drchal, L. Szunyogh, and P. Weinberger, Phys. Rev. B **65**, 125101 (2002).
- ²² P. Soven, Phys. Rev. **156**, 809 (1967).
- ²³ B. Velický, Phys. Rev. **184**, 614 (1969).
- ²⁴ I. Turek, J. Kudrnovský, and V. Drchal, Phys. Rev. B **86**, 014405 (2012).
- ²⁵ I. Turek, J. Kudrnovský, and V. Drchal, Phys. Rev. B **89**, 064405 (2014).

²⁶ R. Kubo, J. Phys. Soc. Jpn. **12**, 570 (1957).

²⁷ A. Bastin, C. Lewiner, O. Betbeder-Matibet, and P. Nozieres, J. Phys. Chem. Solids **32**, 1811 (1971).

²⁸ O. K. Andersen, Phys. Rev. B **12**, 3060 (1975).

²⁹ O. K. Andersen and O. Jepsen, Phys. Rev. Lett. **53**, 2571 (1984).

³⁰ A. Crépieux and P. Bruno, Phys. Rev. B **64**, 014416 (2001).

³¹ K. Carva, I. Turek, J. Kudrnovský, and O. Bengone, Phys. Rev. B **73**, 144421 (2006).

³² O. K. Andersen, Z. Pawłowska, and O. Jepsen, Phys. Rev. B **34**, 5253 (1986).

³³ I. Turek, J. Kudrnovský, and V. Drchal, Phys. Rev. B **92**, 214407 (2015).

³⁴ I. Turek, V. Drchal, J. Kudrnovský, M. Šob, and P. Weinberger, *Electronic Structure of Disordered Alloys, Surfaces and Interfaces* (Kluwer, Boston, 1997).

³⁵ D. Ködderitzsch, K. Chadova, and H. Ebert, Phys. Rev. B **92**, 184415 (2015).

³⁶ K. Fritz, S. Wimmer, H. Ebert, and M. Meinert, Phys. Rev. B **98**, 094433 (2018).

³⁷ T. B. Massalski, ed., *Binary Alloy Phase Diagrams* (American Society for Metals, Metals Park, Ohio, 1986).

³⁸ M.-H. Nguyen, M. Zhao, D. C. Ralph, and R. A. Buhrman, Appl. Phys. Lett. **108**, 242407 (2016).

³⁹ A. Manchon and S. Zhang, Phys. Rev. B **79**, 094422 (2009).

⁴⁰ F. Freimuth, S. Blügel, and Y. Mokrousov, Phys. Rev. B **90**, 174423 (2014).

⁴¹ S. Wimmer, K. Chadova, M. Seemann, D. Ködderitzsch, and H. Ebert, Phys. Rev. B **94**, 054415 (2016).

⁴² I. Turek, J. Kudrnovský, and V. Drchal, in *Electronic Structure and Physical Properties of Solids*, Lecture Notes in Physics, Vol. 535, edited by H. Dreyssé (Springer, Berlin, 2000) p. 349.